Acta Physica Academiae Scientiarum Hungaricae, 53 (1—2), pp. 39—50 (1982)

MODEL FOR THE Mg_1 CENTRE IN NaCl*

A. WATTERICH and K. RAKSÁNYI

RESEARCH LABORATORY FOR CRYSTAL PHYSICS OF THE HUNGARIAN ACADEMY OF SCIENCES
1502 BUDAPEST, HUNGARY

Optical and thermal properties of the Mg_1 centre generated by illumination in the F band of X-irradiated NaCl:Mg crystals have been investigated. A new model of this centre being essentially a dimer which has captured two electrons and two anion vacancies is proposed.

1. Introduction

In Mg^{2+} doped NaCl four different electron excess centres were produced by X-irradiation and subsequent F- and thermal bleaching [1]. The structure of the Mg_1 centre is the least known among them. The Mg_1 centres transform into Mg_2 centres at RT, whereas at higher temperatures the $Mg_2 \rightarrow Mg_3$ centre conversion takes place [1]. Thus the Mg_1 centre can be considered as a primary centre and it would be important to know more about its structure. That is why we tried to follow in more detail the formation kinetics of the Mg_1 centre together with its thermal conversion kinetics. In order to do that the first task was to determine more exactly the optical parameters of the overlapping absorption bands and the optimal conditions and characteristics of the Mg_1 centre formation.

2. Experimental procedures

$MgCl_2$ doped NaCl crystals were grown OH-free by a zone-melting method [2] and cooled down slowly ("as-grown" samples). Some crystals were annealed at 400 °C with subsequent quenching to RT (quenched samples). X-irradiation was carried out at RT using a THX-250 deep-therapy apparatus working at 200 kV and 20 mA yielding a dose rate of ~ 2 C/kg. min. For the bleaching of the F-band at RT a tungsten-iodine lamp equipped with BG-19 and GG-3 filters was used. The optical absorption measurements were recorded at RT by a UNICAM SP-700 spectrophotometer. For the calculations a CDC-3300 computer was used.

* Dedicated to Prof. I. Tarján on his 70th birthday.

3. Experimental results

3.1. The optical parameters

During coloration of "as-grown" crystals in the first stage (i.e. for total irradiation times $t_{irr} < 30$ min) the increase of the F and a V-type band at 209 nm could be observed with a proportionality between the optical densities of both bands (Fig. 1, curve 1).

In the second coloration stage the peak position of the V-band shifted to longer wavelengths and the proportionality changed (Fig. 1, curve 2) indicating the appearance of a new V-type band at longer wavelengths. Also the M band appeared in the optical absorption spectrum.

If the sample was previously annealed at 400 °C for about 10 min and quenched to RT a short X-irradiation and F-bleaching resulted in an optical absorption spectrum showing the presence of a manifold of V bands, the F band (these bands decreased during F-bleaching), and a group of Mg bands between them which increased during F-bleaching (Fig. 2, curve 1). An additional anneal at 100 °C for 10 min yielded curve 2 of Fig. 2. Fig. 2, curve 3 shows the difference spectrum. The group of V band obviously consists of at least two bands: one is unstable at 100 °C (~229 nm), the other (209 nm) being more stable. In the group of Mg bands the Mg_1 band at 332 nm and the one at 390 nm are unstable at 100 °C, and so is the F′ band at 510 nm. Stable bands (Fig. 2, curve 2) in addition to the V band (209 nm) are the Mg_2 (~300 nm) and F (467 nm) bands.

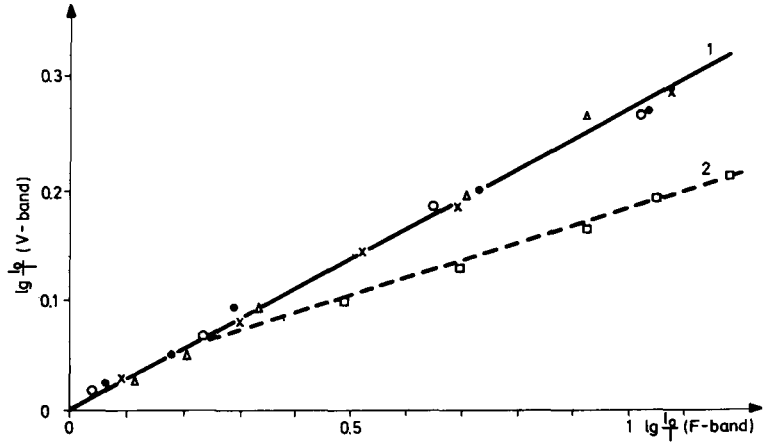

Fig. 1. The optical density of the V band at 209 nm versus that of the F band for the "as-grown" NaCl:Mg crystal

curve 1: First stage of coloration (total irradiation time <30 min; ○, ●, △ and × standing for different samples)

curve 2: Second stage of coloration (the first value was measured after 1 hour of X-irradiation; □)

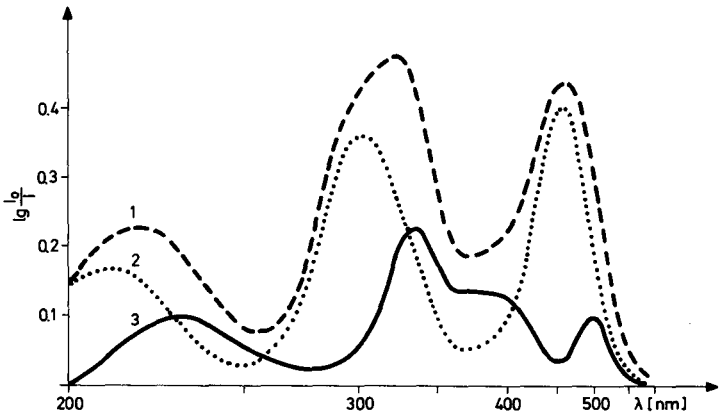

Fig. 2. Curve 1: Optical absorption spectrum of quenched NaCl:Mg after 10 min of X-irradiation and subsequent 10 min of F-bleaching (– – –)
curve 2: The same after an additional 10 min anneal at 100 °C (. . .)
curve 3: The difference of curve 1 and 2 (———)

The original spectrum (Fig. 2, curve 1) was decomposed by an iterative FORTRAN program based on the least square method. The best decomposition was found by assuming seven Gaussian curves (Fig. 3).

In order to determine the parameters of the Mg_3 and Mg_4 bands we used the optical absorption spectrum published earlier [1] (see Fig. 4). In this case the F, V, Mg_2, Mg_3 and Mg_4 bands should be taken into consideration by the decomposition.

All parameters concerning the Mg and V bands obtained from the decompositions are collected in Table I.

The spectrum shown in Fig. 5, curve 1 is mainly the superposition of Mg_3 and Mg_4 bands. Curve 2 belongs to the same sample but annealed at some higher

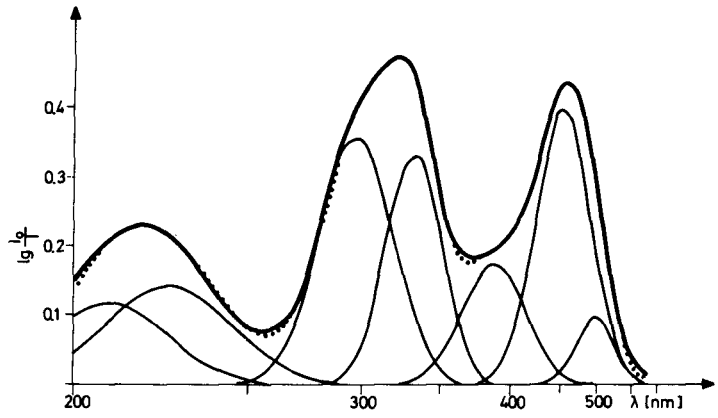

Fig. 3. The Gaussian decomposition of Fig. 2, curve 1 assuming seven Gaussian curves. (Experimental curve: ———, the calculated sum of Gaussian curve: . . . . .)

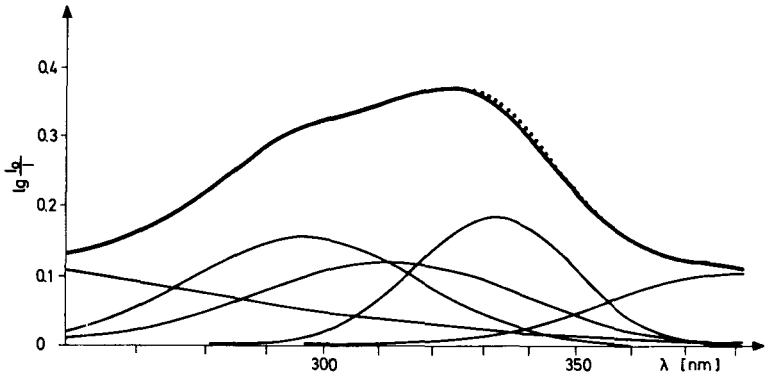

Fig. 4. Optical absorption spectrum of NaCl:Mg after 30 min X-irradiation, F-bleaching for 13 min and annealing at 120 °C for 10 min. (Experimental curve: ———, the calculated sum of Gaussian curves:. . . . .)

temperature (180 °C) where the Mg_3 band becomes unstable. The parameters of the difference (curve 3) are in good agreement with those of the Mg_3 band obtained from the Gaussian decomposition. The calculated parameters of the Mg_4 band are also in good agreement with those given in [3] where the Mg_4 band was prepared independently without the presence of any other interfering Mg band by electrolytical coloration and subsequent "decoloration".

Finally it can be stated that the presence of all the above mentioned absorption bands is experimentally proved and not only assumed for the sake of a good decomposition.

Table I
Parameters of the optical absorption bands obtained from Gaussian decomposition

Centre	Optical absorption peak	
	Position [nm]	Halfwidth [eV]
Mg_1	332±1	0.48±0.01
Mg_2	299±1	0.62±0.01
Mg_3	332±1	0.45±0.01
Mg_4	312±1	0.75±0.01
?	390±1	0.54±0.01
V	209±0.5	1.00±0.01
	226±0.5	1.07±0.01

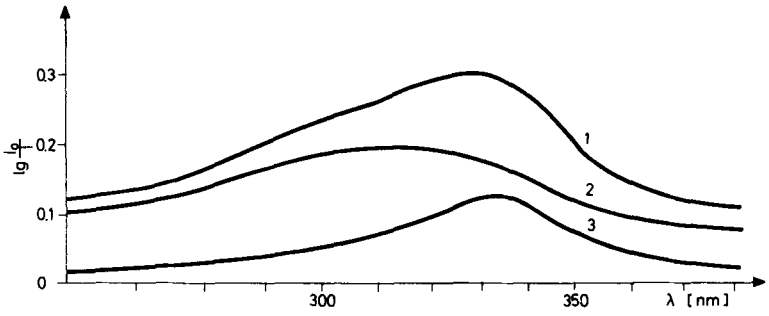

Fig. 5. Curve 1: Optical absorption spectrum of the same crystal as in Fig. 4, but annealed at 120 °C for 30 min
curve 2: The same but heated up to 180 °C
curve 3: The difference of curve 1 and 2

3.2. Optimal conditions and characteristics of the formation of the Mg_1 centre

In order to find out the optimal conditions for a study of the formation kinetics of Mg_1 centres we reinvestigated the "as-grown" crystals.

In "as-grown", X-irradiated and F-bleached crystals (Fig. 6, curve 1) a V band at 209 nm (corresponding to the stabler V band shown in Fig. 3) and a band at ~320 nm, i.e. essentially the Mg_1 band were found. The fact that the latter appears to be asymmetric, shifted and broader than the Mg_1 band found previously by decomposition (Table I) indicates the presence of the Mg_2 band. The extinction of this Mg_2 band, however, is much lower than in the quenched crystal treated similarly (Fig. 6, curve 2). In the "as-grown" crystal neither the F′ nor the 390 nm band appeared.

The spectrum of an "as-grown" crystal X-irradiated as far as the second coloration stage and F-bleached afterwards (Fig. 7) shows only the V, Z_4 like [4], Mg_3 and Mg_4 bands but neither the Mg_1 nor the Mg_2 are present since the Mg_1 band should

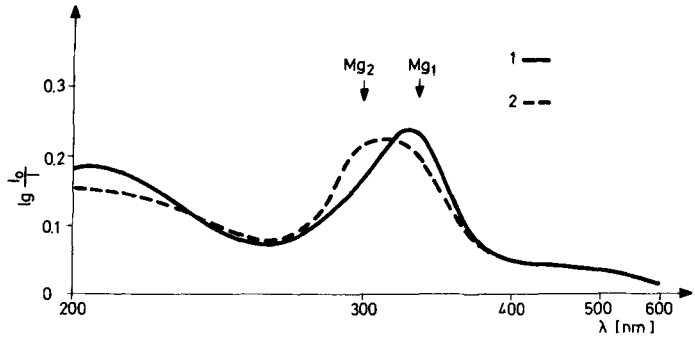

Fig. 6. Optical absorption spectrum of
curve 1: "as-grown" crystal after 10 min of X-irradiation and 10 min of subsequent F-bleaching
curve 2: the same sample but annealed at 400 °C before being treated in the same way as above

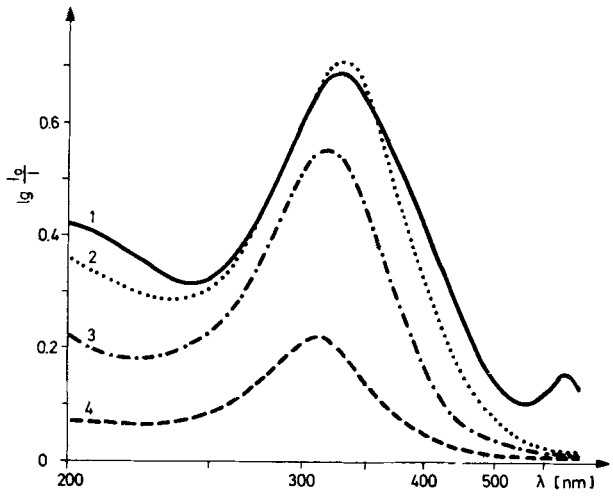

Fig. 7. The optical absorption spectrum of an "as-grown" sample
curve 1: after X-irradiation for 2 hours and total F-bleaching
curve 2: the same with an additional anneal at 100 °C
curve 3: the same with an additional anneal at 150 °C
curve 4: the same with an additional anneal at 180 °C

transform into the Mg_2 band and the Mg_2 band into the Mg_3 band upon annealing at 100 °C and 150 °C, respectively [1], which is not the case in second stage coloured crystals (Fig. 7, curves 1, 2 and 2, 3, respectively). The dominating presence of the Mg_3 centre as opposed to the Mg_2 centre is supported by ESR (their spectra were identified in [1]).

Consequently, the formation kinetics of the Mg_1 band can be best studied using "as-grown" crystals X-irradiated in the first coloration stage ($t_{irr} < 30$ min). In this case only the changes of the V (209 nm), Mg_1, Mg_2 and F bands during F-bleaching have to be taken into account.

Thus we chose such crystals with $t_{irr} = 20$ min and recorded the optical extinction at the peak maxima shown in Table I between short F-bleaching steps. For the evaluation of the spectra a FORTRAN decomposition program was used assuming Gaussian forms for the V, Mg_1 and Mg_2 bands and the real form (as observed before F-bleaching) for the F band. This was necessary due to the asymmetric shape of the F band at the centre concentration used.

The interdependence of extinctions in Mg and F bands during F-bleaching is shown in Fig. 8. In the process of the Mg_1 band formation three stages could be distinguished: in the first (beginning) stage the F band decreases rapidly and the Mg_1 band increases very slowly. In the second stage the increase of the Mg_1 band becomes more rapid, in the third (final) stage slower again. The smaller the Mg concentration the slower the formation rate in the last stage (Figs 8 and 9a).

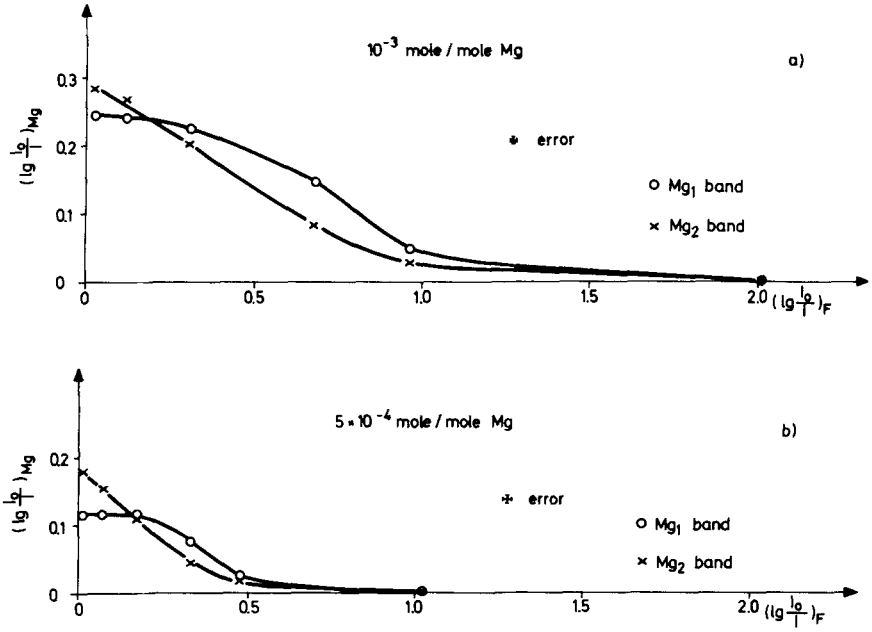

Fig. 8. Optical density of the Mg_1 and Mg_2 bands versus that of the F band during F-bleaching of "as-grown" and X-irradiated NaCl:Mg. (Decomposition-corrected values in the band maxima listed in Table I)

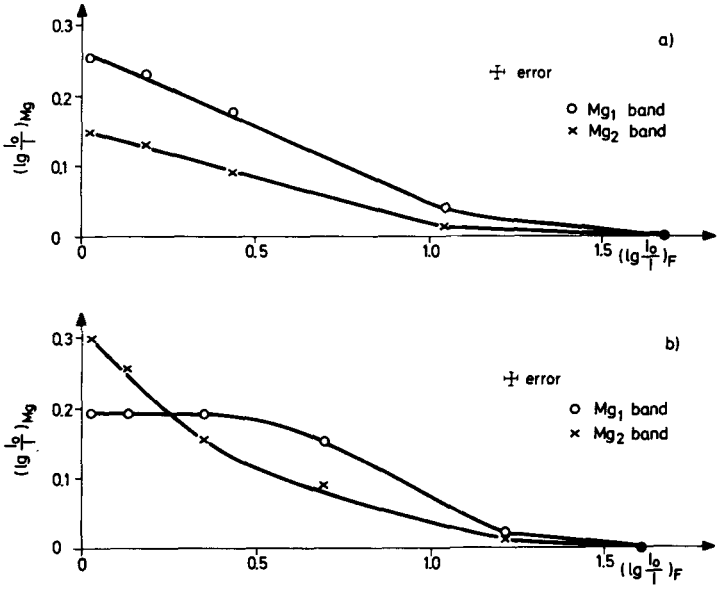

Fig. 9. Optical density of the Mg_1 band versus that of the F band during F-bleaching. The same sample was used in "as-grown" a) and quenched b) cases. The Mg concentration was 3×10^{-3} mole/mole

Comparing the third stages of "as-grown" and quenched crystals it can be seen that in the second case the extinction of the Mg_1 band saturates (Fig. 9). This effect is very similar to that observed in an "as-grown" crystal with small Mg concentration (Fig. 8b). In a quenched crystal the saturation of the Mg_1 extinction is accompanied by the increased formation rate of the Mg_2 band.

3.3. The thermal conversion of the Mg_1 band

The $Mg_1 \rightarrow Mg_2$ thermal conversion was also quantitatively followed.

As it was already established [1] at the end of this conversion a small Mg_3 band is also present in the spectrum. Since the peak positions of the Mg_1 and Mg_3, on the one hand, and Mg_2 and Mg_4 bands, on the other hand, are rather close to each other (Table I), it is hard to decide whether the Mg_3 and Mg_4 bands exist immediately after F-bleaching. We know, however, that X-irradiation in the second stage promotes the formation of the Mg_3 and Mg_4 bands (Fig. 7) though in the present case only first stage coloration was applied. Moreover, Mg_1 and Mg_3 bands have different optical conversion characteristics: as a result of optical bleaching the Mg_1 centres are converted into F centres, in contrast to the case of the Mg_3 centres which recombine with V centres [1].

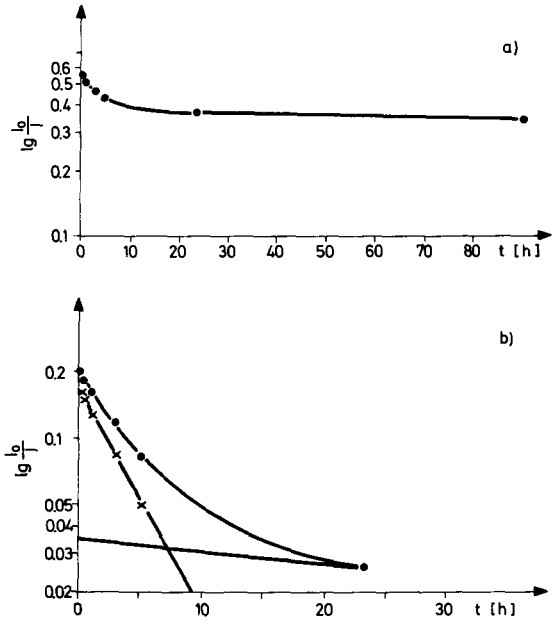

Fig. 10. a) The optical density of the Mg_1 band versus storing time. (The sample was kept in the dark at RT). b) The last measured value in Fig. 10a was subtracted from all the other values (. . .). This curve could be easily fitted by the sum of two linear functions

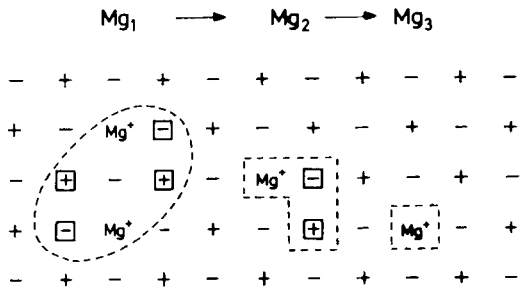

Fig. 11. The models of the Mg centres

Taking into account these properties an upper limit for the extinction of the Mg_3 band immediately after F-bleaching could be given: no more than 15% of the whole extinction at 332 nm belongs to the Mg_3 band.

During thermal bleaching the whole extinction was measured at 332 nm (E_{332}) and drawn versus storing time (Fig. 10a). This consists of the whole extinction of the Mg_1 and Mg_3 bands and a certain contribution (a) of that of the Mg_2 band:

$$E_{332} = E_1 + aE_2 + E_3 , \tag{1}$$

where E_i's are the extinctions of the corresponding Mg bands at the band maxima.

The conversions are assumed to be of first order. This seems to be quite plausible for $Mg_2 \rightarrow Mg_3$ (see the models in Fig. 11), but questionable for $Mg_1 \rightarrow Mg_2$. Some justification for this assumption is provided by the successful fitting procedure to be presented.

The facts that no back-conversions could be detected and both the Mg_1 and Mg_2 decompositions appeared to be full indicate that back-reactions can be neglected at the present stage.

The changes of the extinctions were described by the following differential equations:

$$\frac{dE_1}{dt} = -k_1 E_1 , \tag{2}$$

$$\frac{dE_2}{dt} = \alpha k_1 E_1 - k_2 E_2 , \tag{3}$$

$$\frac{dE_3}{dt} = \beta k_2 E_2 , \tag{4}$$

where the k_i's are the rate constants of the corresponding conversion processes, the parameters α and β relating the extinctions of various bands during conversion.

Solving the differential equations (2—4) and substituting the solution into (1) the final solution is

$$E_{332}(t)=E'e^{-k_1t}+E''e^{-k_2t}+E''', \tag{5}$$

where E', E'' and E''' are parameters. The value of E''' was determined from the last point of Fig. 10a. Subtracting this from all experimental values the curve in Fig. 10b was obtained. This could be easily fitted by two exponentials. Consequently, Eq. (5) described the process quite well and therefore the assumption concerning the first order kinetics of the Mg_1 band conversion is not in contradiction with the experiment.

4. Discussion

Table II contains all characteristics which should be taken into consideration in the creation of a new model for the Mg_1 centre, more suitable than the one proposed in [1].

The decrease of the formation rate in the last stage cannot be explained only by the instability of the Mg_1 band at RT. This effect together with its dependence on Mg concentration indicates the presence of a precentre obviously connected with the dopant. These precentres might exist in the crystal prior to F-bleaching and are used up during illumination simultaneously with the increase of the formation rate of the Mg_2 band.

Applying a large dose of X-irradiation the Mg_1 band formation saturates very early during F-bleaching either because of the small concentration of the precentres

Table II

Main characteristics of the Mg_1 centre

The Mg_1 centre	
is not paramagnetic	
can be converted by	optical bleaching →F centre
	X-reirradiation →F centre
	thermal bleaching →Mg_2 centre (first order kinetics)
formation is promoted by the circumstances	large Mg concentration
	"as-grown" crystal
	first stage X-irradiation
formation has stages	I slow
	II rapid
	III slow

compared to the F centre concentration, or because long irradiation destroys the precentres themselves.

On the other hand the slow first stage in the formation of the Mg_1 centre indicates that a second precentre should also exist which should be formed during F-bleaching.

The Mg^{2+} ions, like other divalent impurities are built in the crystal together with charge-compensating cation vacancies forming dipoles. The dipoles aggregate into polymers, in the simplest case into dimers the existence of which is proved [5—8].

The experimental facts that:

1. the formation of the Mg_1 centres saturates in quenched crystals (Fig. 9),

2. the long X-irradiation does not promote the formation of Mg_1 centres suggest that the above mentioned first precentre is some kind of aggregated dipoles. In fact, annealing decreases the concentration of polymers [9], and X-irradiation destroys in several cases the divalent metal aggregates [10]. The results concerning this disaggregation effect for the NaCl:Mg system are as follows: X-irradiation

1. disaggregates the $MgCl_2$ precipitate,

2. decreases the concentration of Mg—Mn dimers,

3. probably dissociates the dipoles. (This conclusion may be drawn from the fact that in NaCl:Mg crystals V_F-type centres could be measured by ESR similar to that found in NaCl:Ca [11]. The formation of V_F-type centres is probably connected to the appearance of free cation vacancies.)

The simplest assumption for the first precentre is a dimer. Dimers exist in "as-grown" crystals but annealing and long X-irradiation destroy them. In these cases Mg_1 centres are formed in smaller concentration.

The most plausible assumption for the second precentre (which should be formed during F-bleaching) is an anion vacancy. This view is supported by the observation that the Mg_2 centre formation also requires this precentre (see Figs. 8 and 9) and indeed the anion vacancy is one of the components of the Mg_2 centre according to our model based on other experiments.

Taking into account the above mentioned precentres and the lack of ESR signal the new and more convenient model for the Mg_1 centre is: one dimer + two anion vacancies + two electrons (Fig. 11). Electron excess dimer centres (including or not cation vacancies) are well known also in other systems like Ag_2^+ in KCl [12], $(Cd^+)_2$ in KCl [13] and Tl_2^+ and Ga_2^+ in KCl [14].

The above model is supported by the experience concerning the first order kinetics of the thermal decomposition of the Mg_1 centre and in conversion into Mg_2 centre: one Mg_1 centre dissociates into two Mg_2 centres.

The larger stability of the Mg_2 centre compared to that of the Mg_1 centre can be explained also very well on the basis of the above model. The jump of a cation vacancy needs smaller energy than the moving of a whole vacancy-pair [15]. A vacancy jump can dissociate the Mg_1 centre whereas the same vacancy jump does not lead to

structural change in the Mg_2 centre, only the orientation of the vacancy pair changes. The decomposition of the Mg_2 centre occurs when the whole vacancy pair moves away.

The new model of the Mg_1 centre explains all the experiments without any contradiction.

References

1. A . Watterich and R. Voszka, Acta Phys. Hung., **33**, 323, 1973.
2. R. Voszka, I. Tarján, L. Berkes and J. Krajsovszky, Kristall und Technik, **1**, 423, 1966.
3. R. Voszka and A. Watterich, phys. stat. sol. (b), **55**, 787, 1973.
4. A. Watterich, Phys. Stat. Sol. (b), **88**, K51, 1978.
5. R. Capelletti, Proceedings of the Symp. on Thermal and Photostimulated Currents in Insulators (ed. by D. M. Smyth) p. 1, 1976.
6. M. Ikeya and J. H. Crawford, Phys. Stat. Sol. (b), **58**, 643, 1973.
7. S. Unger and M. M. Perlman, Phys. Rev., B **10**, 3692, 1974.
8. G. Berg, F. Fröhlich and S. Siebenhüner, Phys. Stat. Sol. (a), **31**, 385, 1975.
9. M. Hartmanová, phys. stat. sol. (a), **7**, 303, 1971.
10. A. Watterich and R. Voszka, Phys. Stat. Sol (b), **93**, K161 (1979).
11. A. Watterich, M. Gécs and R. Voszka, Phys. Stat. Sol., **31**, 571, 1969.
12. R. A. Zhitnikov, P. G. Baranov and N. I. Melnikov, Phys. Stat. Sol. (b), **59**, K111, 1973.
13. L. Bern-Dor, A. Glasner and S. Zolotov, J. Sol. St. Chem., **4**, 4, 1972.
14. V. S. Osminin and S. G. Zazubovich, Opt. i Spektr., **29**, 924, 1975.
15. M. Beniere, M. Chemla and F. Beniere, J. Phys. Chem. Solids, **37**, 525, 1976.